

Simple and Precise Quantification of Iron Catalyst Content in Carbon Nanotubes Using UV/Visible Spectroscopy

Elsye Agustina, Jeungchoon Goak, Suntae Lee, Youngho Seo, Jun-Young Park, and Naesung Lee*^[a]

Iron catalysts have been used widely for the mass production of carbon nanotubes (CNTs) with high yield. In this study, UV/visible spectroscopy was used to determine the Fe catalyst content in CNTs using a colorimetric technique. Fe ions in solution form red–orange complexes with 1,10-phenanthroline, producing an absorption peak at $\lambda = 510$ nm, the intensity of which is proportional to the solution Fe concentration. A series of standard Fe solutions were formulated to establish the relationship between optical absorbance and Fe concentration. Many Fe catalysts were microscopically observed to be en-

cased by graphitic layers, thus preventing their extraction. Fe catalyst dissolution from CNTs was investigated with various single and mixed acids, and Fe concentration was found to be highest with CNTs being held at reflux in HClO₄/HNO₃ and H₂SO₄/HNO₃ mixtures. This novel colorimetric method to measure Fe concentrations by UV/Vis spectroscopy was validated by inductively coupled plasma optical emission spectroscopy, indicating its reliability and applicability to assess Fe content in CNTs.

Introduction

Since the discovery of carbon nanotubes (CNTs), a number of applications have been studied to take advantage of their superior thermal,^[1] mechanical,^[2] and electronic properties.^[3] CNTs have been highlighted as promising materials for applications such as composites,^[4] supercapacitors,^[5] and gas and toxin sensors in the food industry, military, and environmental fields;^[6] for these applications, CNTs have been mass produced by chemical vapor deposition (CVD).^[7,8] Increasing the production yield of CNTs requires a combination of catalysts and supports,^[7,9] and iron (Fe) catalysts on alumina supports have been used successfully for mass production.^[10] However, the presence of Fe catalysts in as-produced CNTs may limit performance in some applications, such as chemical sensors^[11] and semiconducting composites for high-voltage power cables.^[12] Even trace concentrations of metal ions can cause data misinterpretation in the former and electrical breakdown in the latter. This significant catalyst involvement in redox activity has been detected through hydrogen peroxide electrocatalysis examination^[13] and electrochemical activity demonstrations using Fe-rich CNTs.^[14]

High-purity CNTs have been created by investigating the synthesis^[15] or purification process,^[16] and a simple and precise

analytical method is needed to determine the often very low concentrations of metals in these CNTs. Several methods have been used to measure metal concentrations, such as thermogravimetric analysis (TGA), energy-dispersive X-ray spectroscopy (EDX), X-ray fluorescence spectrometry (XRF), inductive coupled plasma optical emission spectroscopy (ICP-OES), inductive coupled plasma mass spectrometry (ICP-MS), and neutron activation analysis (NAA).^[17] TGA is a simple and widely available method, providing a total ash content consisting of metal carbides or oxides.^[18] When the residue obtained from TGA was analyzed by X-ray diffraction, the metallic impurities were identifiable in the form of carbides or oxides as well.^[19] EDX is able to identify elements, but its measurement of concentration is inaccurate due to the small scanning area. XRF is simple and quick and does not require sample preparation, but it does require a large sample volume (~0.1 g).^[20] Among the available analytical tools, NAA is the most advanced and accurate tool for determining metals at low concentrations, is highly sensitive, and requires no sample preparation. Ge et al.^[21,22] used ICP-MS to analyze metal impurities in CNTs with high detection sensitivity. Yang et al.^[23] used both ICP-MS and ICP-OES for the same purpose. However, this sophisticated method is expensive, time-consuming, and not widely available.

Ultraviolet-visible (UV/Vis) spectroscopy can be used as an alternative tool for measuring low metal concentrations, and has the advantages of low cost, ease in handling, wide availability, and high sensitivity. UV/Vis spectroscopy detects the light absorption of molecules with non-bonding electrons or π -electrons.^[24] Fe, a major catalyst for CNT production, is a transition metal unsuitable for detection by UV/Vis spectroscopy. Therefore, chemical modification is required to measure Fe concentrations using a UV/Vis spectrometer. Fe cations natural-

[a] E. Agustina, Dr. J. Goak, S. Lee, Prof. Y. Seo, Prof. J.-Y. Park, Prof. N. Lee Hybrid Materials Center (HMC), Department of Nanotechnology and Advanced Materials Engineering, Sejong University 209 Neungdong-ro, Gwangjin-gu, Seoul 143-747 (Republic of Korea) E-mail: nslee@sejong.ac.kr

© 2015 The Authors. Published by Wiley-VCH Verlag GmbH & Co. KGaA. This is an open access article under the terms of the Creative Commons Attribution-NonCommercial-NoDerivs License, which permits use and distribution in any medium, provided the original work is properly cited, the use is non-commercial and no modifications or adaptations are made.

ly form coordination complexes with molecules containing π -electrons (ligands). One of the most prominent ligands for Fe complexes is phenanthroline (phen).^[25] This bidentate chelating agent has two nitrogen atoms at the *ortho* positions of the rigid half-ring structure. The lone pair electrons of the nitrogen atoms coordinate with Fe^{2+} cations. The resulting Fe–phen complex has an absorbance at a specific wavelength, with the peak intensity proportional to the Fe cation concentration in the sample. The use of phen as a chelating agent has advantages due to its wide commercial availability and low cost relative to other Fe-coordinating spectrometric ligands such as *N,N'*-ethylenebis(ethanesulfonamide),^[26] ferrozine, and ammonium pyrrolidinedithiocarbamate (APDC). Furthermore, quantitative analysis of Fe using phen has been conducted in waste water and tissue homogenates.^[27] This method has also been proposed for environmentally friendly portable lab-on-paper devices,^[28] Fe recycling in Fe-rich sludge,^[29] and biological applications such as chelation to prevent Fe toxicity during hemorrhaging.^[30] The interaction between phen and CNTs has also been suggested for selective recognition of copper and hydrogen peroxide sensing.^[31]

This study assessed a simple and precise method for quantitative measurement of Fe concentrations in CNTs using UV/Vis spectroscopy. A procedure for sample preparation and Fe analysis using UV/Vis spectroscopy was developed by modifying the established procedure to form a Fe–phen complex from Fe catalyst residues in CNTs which displays a red–orange color in aqueous solution.^[32] A calibration relationship between optical absorbance and Fe concentration was constructed by using a series of standard Fe solutions of known concentrations. The absorption of the Fe–phen complex at a visible wavelength increased linearly with increasing Fe–phen concentration in solution;^[24] hence, Fe concentrations in an unknown solution may be evaluated easily and accurately. This study also assessed optimized acid reflux conditions for complete extraction of Fe from CNTs for accurate measurement of Fe concentrations. The colorimetric method using UV/Vis spectroscopy was verified by confirming Fe concentrations using ICP-OES. To our knowledge, this study is the first to report that the Fe content of CNTs can be accurately measured with a simple, reliable, and readily available UV/Vis spectroscopic technique.

Results and Discussion

Figure 1 shows the CNT-A used to develop the Fe content determination method. Scanning electron microscopy (SEM) shows non-bundled and individually separated tubes, but some degree of entanglement appeared between the structures (Figure 1 a). Transmission electron microscopy (TEM) reveals multi-layered tubes with an average diameter of 15.5 ± 4.79 nm, which was calculated from 90 nanotubes (Figure 1 b). Metal catalyst particles were usually enclosed by thick graphitic layers (Figure 1 c); the graphitic layer should be removed or at least cracked so that etchants may access and eliminate these metallic impurities. Raman spectra (not shown) of the CNTs had an average intensity ratio of the G and D bands (I_G/I_D) of 0.76 ± 0.04 , indicating that they possess quite low crystallinity.

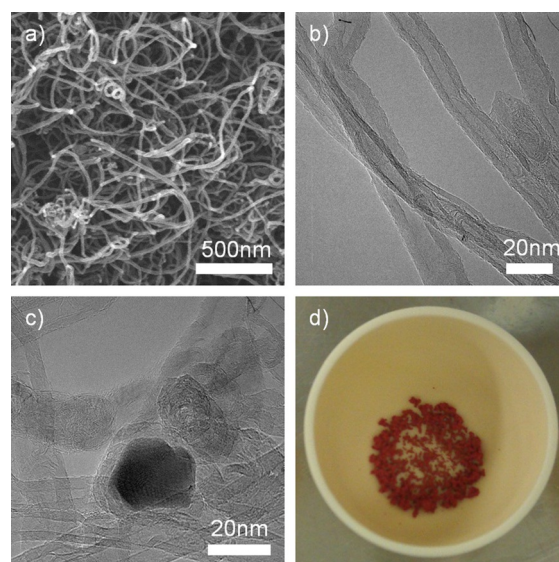
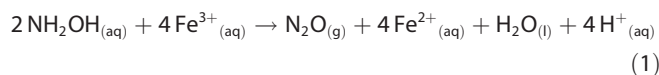


Figure 1. a) SEM and b) TEM images of CNTs. TEM images show their multi-layered structure and an average diameter of 15.5 nm, calculated from 90 nanotubes. c) TEM image of a metal particle encapsulated in multiple graphitic layers. d) Red-colored ash formed by oxidizing CNTs at 900 °C, 3.51 % by weight, taken by a digital camera.

In a derivative of the TGA curve (not shown), the oxidation peak temperature of the CNTs was ~ 650 °C. A 3-g sample of AP-CNTs was burned at 900 °C in air to completely remove all carbonaceous material, and the ashes obtained were 3.51 wt.% of the CNTs. As shown in Figure 1 d, the ashes were red in color, indicating that iron oxide was formed while burning the CNTs in air.

In this spectrometric study, divalent Fe ions (Fe^{2+}) formed a red–orange Fe–phen complex with a tricyclic organic ligand, 1,10-phenanthroline.^[25] For stable formation of the Fe–phen complex, known as ferrioin,^[33] the acidity of the aqueous solution should be kept in the pH 4–7 range by adding a sodium acetate buffer solution.^[34–36] At acidities below pH 3, the red color of the solution vanishes; above pH 7, Fe ions precipitate as iron hydroxide.^[33] Under atmospheric conditions, stable trivalent Fe ions (Fe^{3+}) are usually produced. Hydroxylamine as a reducing agent converts the valence state of Fe ions from trivalent (Fe^{3+}) to divalent (Fe^{2+}). The reduction mechanism for Fe ions has been suggested as [Equation (1)]:^[37]



Phen then reacts with Fe^{2+} to form the red–orange colored Fe–phen complex, by the reaction shown in Figure 2 a.

A series of standard Fe–phen complex solutions with Fe concentrations of 1–9 ppm were made, and a photograph of these solutions is presented in Figure 2 b. The solution visibly reddened with increasing Fe concentration. Absorption spectra for these solutions, measured in the visible spectral range of $\lambda = 400$ –600 nm, exhibited absorption peaks at $\lambda = 510$ nm (Figure 2 c).^[38] According to the Lambert–Beer law,^[24] a linear

relationship was drawn between the Fe concentrations of the solutions and the corresponding maximum absorbance values, as shown in Figure 2d, in which the linearity, indicated by the R^2 value, is very close to 1. The equation obtained from linear regression was used to calculate the Fe concentration of an unknown solution by measuring the maximum absorbance value in its absorption spectrum.

Our AP-CNTs were synthesized by CVD with an Fe catalyst embedded on alumina supports. Because the solutions prepared for analysis of Fe impurities may therefore also contain Al impurities, it was necessary to confirm whether the presence of Al ions in the solution has any influence on the formation of Fe–phen complexes, to ensure the assessment of Fe concentrations is accurate. Solutions were prepared by mixing the pure Fe and Al solutions and then by following the procedure for formation of Fe–phen complexes. Fe concentrations were measured in these solutions by UV/Vis spectroscopy. Figure 2e shows that the constructed and measured Fe concentrations were a nearly exact match for each other, with negligible deviation. This indicates that the Fe concentration can be

precisely detected without disturbance from Al ions in solution, a finding that is consistent with previous studies.^[39,40]

Figure 2d shows the calibration equation for Fe concentrations from 0 to 9 ppm. If the prepared solution has a higher Fe concentration, it must be diluted to within this detection range. Actual Fe concentrations [Fe] in the AP-CNTs can be simply calculated from Fe concentrations measured for the diluted solution prepared using CNTs or ash, as follows:

$$\text{CNT [Fe]} = \frac{m_{\text{Fe}}}{m_{\text{CNT}}} = DF \frac{C_{\text{Fe}} \cdot V_i}{m_{\text{CNT}}} = DF \frac{C_{\text{Fe}} \cdot V_i}{m_{\text{ash}}} R_{\text{ash}}$$

$$\text{where } DF = \frac{V_1}{V_i} \cdot \frac{V_f}{V_2} \quad (2)$$

$$\text{and } R_{\text{ash}} = \frac{m_{\text{ash}}}{m_{\text{CNT}}}$$

Here, m_{CNT} and m_{Fe} are the masses of the AP-CNTs, including metallic impurities and Fe, respectively, expressed in grams. DF stands for a dilution factor, which indicates how many times the solution is diluted to fall within the Fe detection range of

0–9 ppm. In our experiment, dilution was conducted in two steps: diluting a 10 mL (V_i) acid solution in a 100 mL volumetric flask (V_1) followed by a second dilution obtained by sampling a 5 mL (V_2) volume taken from V_1 in a 50 mL volumetric flask (V_f). Thus, a DF value of 100 was obtained for our experiment. C_{Fe} is the Fe concentration of the diluted solution expressed in ppm ($\mu\text{g mL}^{-1}$), which is calculated by inputting the absorbance value of an unknown solution into the calibration equation given in Figure 2d. R_{ash} is the ratio of the ash mass (m_{ash}) of the AP-CNTs to the AP-CNT mass (m_{CNT}).

For ICP-OES measurement, CNTs are usually held at reflux in a strong acid. The Fe concentration in the acid solution may vary depending on how completely the metal impurities are dissolved. The dissolution of metal impurities can also be affected by various factors such as the morphology and volume of CNTs dissolved, acid type, reflux temperature, and time, so the acid reflux conditions should be optimized for accurate Fe analysis. Aqua regia, $\text{HCl}/\text{HNO}_3 = 3:1$, was used in this study to dissolve metal catalysts in the CNTs because it is a strong oxidant

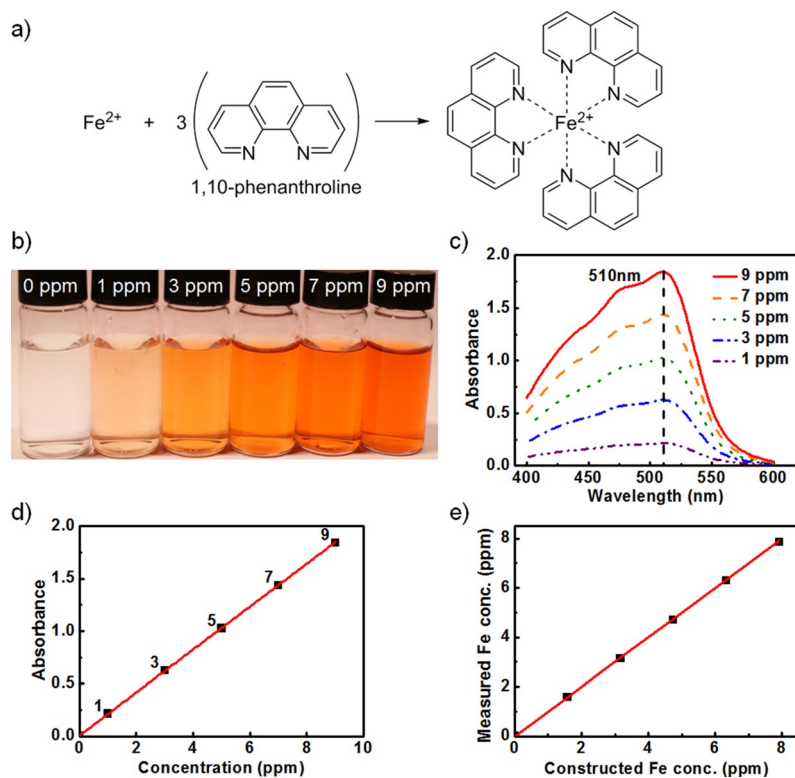


Figure 2. a) Scheme of Fe–phen complex formation; coordination of an Fe^{2+} ion with three phen molecules via lone-pair electrons on the N atoms of phen. b) Standard solutions of Fe–phen complex used for calibration, containing Fe concentrations from 0–9 ppm, taken by a digital camera. The red–orange color of the solutions becomes stronger as the Fe concentration increases. c) Absorption spectra of the standard solutions in the visible spectral range, measured by UV/Vis spectroscopy. d) Linear relationship between optical absorbance and Fe concentration for the standard solutions. The absorbance was measured at the maximum peak position of 510 nm for the absorption spectra shown in panel c. Linear fitting: $A = 0.20423C + 0.00716$, $R^2 = 0.99994$. The coefficient of determination to designate linearity is calculated using $R^2 = \frac{\sum (\bar{y} - \hat{y}_i)^2}{\sum (y_i - \bar{y})^2}$. Here, y_i is the observed absorbance value, \bar{y} is the mean absorbance, and \hat{y}_i is the fitted absorbance value. e) Fe concentrations were measured at the maximum peak position of 510 nm for the absorption spectra shown in panel c. Linear fitting: $y = 0.99114x + 0.00701$, $R^2 = 0.99998$.

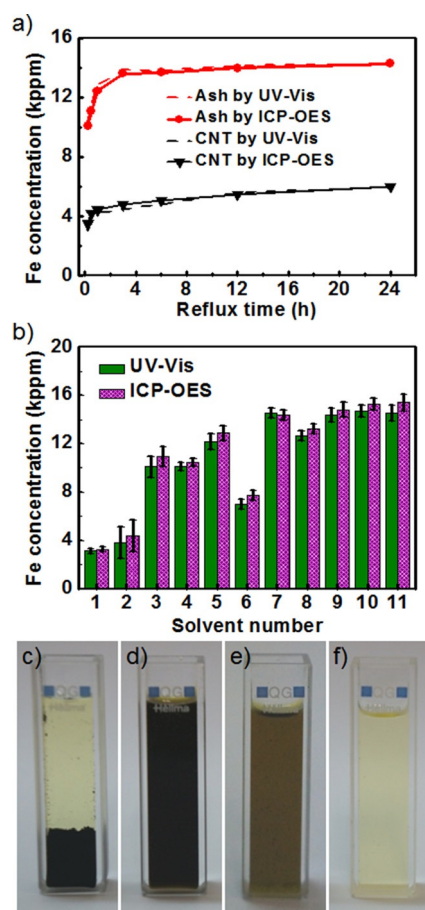


Figure 3. Comparison of Fe concentrations measured by UV/Vis spectroscopy and ICP-OES for the solutions prepared by treating a) CNTs and ash in the HCl/HNO₃ (3:1) mixture as a function of reflux time and b) CNTs in various single and mixed acid solvents for 6 h. Solvent numbers are denoted as follows (mixture ratios as v/v): 1. H₂SO₄, 2. HCl, 3. HNO₃, 4. f-HNO₃, 5. HClO₄, 6. HCl/HNO₃ (3:1), 7. H₂SO₄/HNO₃ (3:1), 8. HClO₄/HNO₃ (1:3), 9. HClO₄/HNO₃ (1:1), 10. HClO₄/HNO₃ (3:1), 11. HClO₄/f-HNO₃ (3:1). Data are the average ± SD of three independent measurements. c)–f) Images of solutions taken by digital camera after holding CNTs at reflux for 6 h in acid mixtures of c) HCl/HNO₃ (3:1), d) H₂SO₄/HNO₃ (3:1), e) HClO₄/HNO₃ (3:1), and f) HClO₄/f-HNO₃ (3:1).

that is frequently used to purify CNTs through liquid oxidation.^[41] Figure 3a shows Fe concentrations extracted by aqua regia from the CNTs and ashes as a function of reflux time. For these same solutions, the Fe concentrations were measured by UV/Vis spectroscopy (solid lines in Figure 3a) and ICP-OES (dashed lines in Figure 3a), which are in good agreement with each other (Figure 3a). The colorimetric method using UV/Vis spectroscopy is reliable and applicable for assessing Fe content in CNTs and ashes, as confirmed by ICP-OES.

In Figure 3a, the Fe concentration in the CNTs was threefold lower than that in the ashes. This considerable difference is probably because the Fe catalysts in the CNTs were not completely dissolved during reflux in acid. Figure 3c shows an image of the solution taken after the CNTs were held at reflux in aqua regia for 6 h, where carbon precipitates were clearly observed at the bottom of the cell due to incomplete dissolution. This indicates that aqua regia has insufficient oxidizing

power to dissolve all CNT materials, and thus Fe catalysts within the CNTs or encapsulated in graphitic layers (Figure 1c) were not dissolved during the acid reflux. Aqua regia is a strong oxidant, but gradually loses its strength by releasing oxidative compounds in the form of nitrosyl chlorides and chlorine gas.^[42] Stronger oxidant acids that are capable of etching away further CNT materials and graphitic layers are required to completely dissolve Fe catalysts that may be encapsulated by CNTs or graphitic layers.

Five single acids and six acid mixtures were examined to compare their extraction powers for Fe catalysts from the AP-CNTs (Figure 3b). The acid reflux was performed for 6 h in all cases, as the Fe concentration increased rapidly for a reflux time of 0–2 h and was observed to nearly plateau at 6 h in aqua regia (Figure 3a). The Fe concentrations of the refluxed solutions were analyzed using both UV/Vis spectroscopy and ICP-OES. The five bar graphs, 1 to 5 in Figure 3b, show the solution Fe concentrations after reflux by single concentrated acids: H₂SO₄, HCl, HNO₃, fumed-HNO₃ (f-HNO₃), and HClO₄. From the UV/Vis spectrometric measurements, Fe concentrations, stated with their uncertainty^[43] from measurement process, were 3.13 ± 0.12 and 3.79 ± 0.13 kppm for the H₂SO₄- and HCl-refluxed solutions, respectively, but reached 10.09 ± 0.13 and 12.14 ± 0.14 kppm for the HNO₃- and HClO₄-refluxed solutions, respectively. Fe concentrations for HNO₃ (70%) or f-HNO₃ (93%) were observed at similar levels, 10.30 ± 0.13 kppm, for the 6 h reflux, but the reflux appeared to progress more rapidly for f-HNO₃. HClO₄, a strong oxidizing agent with oxidation power originating from the perchlorate ion (ClO₄⁻), was capable of extracting an Fe concentration of 12.14 ± 0.13 kppm from the CNTs. In treatments with single acids, HCl and H₂SO₄ were less oxidative in digesting the CNTs and graphitic layers. The ability to fully etch carbon materials seems to be closely related to the oxidizing nature of an acid rather than its acidic strength.^[44] Among the single acids tested, HNO₃ and HClO₄ are considered to be powerful oxidants, and effective for extracting Fe catalysts from CNTs. Nevertheless, none of the single acids were able to completely digest the CNTs, because black precipitates were observed in all solutions after reflux with single acids.

Because HClO₄ and HNO₃ exhibited the strongest extraction capacity among the single acids, they were mixed together to enhance their oxidizing power. HClO₄ and HNO₃ mixtures were prepared at three different ratios of 1:3, 1:1, and 3:1. As shown in Figure 3b, the HClO₄/HNO₃ mixtures resulted in Fe concentrations of 12.62 ± 0.14 , 14.38 ± 0.14 , and 14.68 ± 0.14 kppm for ratios of 1:3, 1:1, and 3:1 in the 6 h reflux experiments, respectively. More Fe catalyst was extracted as the HClO₄ fraction was increased in the HClO₄/HNO₃ mixture. Among the three HClO₄/HNO₃ mixtures, the strongest acid mixture, 3:1, produced a semitransparent brown solution upon reflux of the CNTs for 6 h (Figure 3e), indicating that the CNTs were almost dissolved in this mixture, but not completely. For further dissolution of the CNTs, HNO₃ was replaced with f-HNO₃ in a HClO₄/f-HNO₃ ratio of 3:1. As shown in Figure 3f, a transparent solution was obtained without any trace of the CNTs for this acid mixture after 6 h, suggesting that the AP-CNTs were complete-

ly dissolved, and all Fe catalysts were extracted. In this acid mixture, the Fe concentration was 14.52 ± 0.14 kppm.

We also investigated a $\text{H}_2\text{SO}_4/\text{HNO}_3$ mixture (3:1), which has been widely used for the oxidation of CNTs.^[45] The refluxed solution contained Fe concentrations as high as 14.56 ± 0.14 kppm, but showed a dark-brown color, as depicted in Figure 3d. H_2SO_4 alone had the weakest Fe extraction capacity among the single acids examined, but exhibited a synergetic effect when mixed with HNO_3 in a 3:1 ratio. As shown in Figure 3b, the $\text{H}_2\text{SO}_4/\text{HNO}_3$ (3:1), $\text{HClO}_4/\text{HNO}_3$ (1:1), $\text{HClO}_4/\text{HNO}_3$ (3:1), and $\text{HClO}_4/\text{f-HNO}_3$ (3:1) mixtures yielded similar Fe concentrations of 14.56 ± 0.14 , 14.38 ± 0.14 , 14.67 ± 0.14 , and 14.52 ± 0.14 kppm, respectively, but only the $\text{HClO}_4/\text{f-HNO}_3$ (3:1) mixture produced a transparent and clear solution. During acid reflux, complete Fe extraction depends on the destruction of CNTs or graphitic layers enclosing the Fe catalysts. It seems that $\text{H}_2\text{SO}_4/\text{HNO}_3$ (3:1), $\text{HClO}_4/\text{HNO}_3$ (1:1), and $\text{HClO}_4/\text{HNO}_3$ (3:1) mixtures destroyed or cracked all CNTs or graphitic layers such that the encapsulated Fe catalysts could be extracted, whereas the $\text{HClO}_4/\text{f-HNO}_3$ (3:1) mixture totally destroyed all carbon materials. Hence, the four mixtures tested are almost equally powerful for Fe extraction from CNTs, but $\text{HClO}_4/\text{f-HNO}_3$ (3:1) is superior to the others in consuming the carbon materials during reflux.

Nitric acid is thought to digest carbon materials via a nitration process with nitronium (NO_2^+) ions. According to a computational study by Gerber et al.,^[46] nitronium ions first attack the most reactive carbon atoms on surface defects, and produce and then enlarge the vacancies for a prolonged reaction time. In concentrated nitric acid, nitronium ions form through equilibrium self-dissociation according to the following reaction: $2\text{HNO}_3 \rightarrow \text{NO}_2^+ + \text{NO}_3^- + \text{H}_2\text{O}$.^[47] The formation of these particular ions can be accelerated by adding a strong acid such as sulfuric or perchloric acid.^[48] The reactions are $\text{HNO}_3 + 2\text{H}_2\text{SO}_4 \rightarrow \text{NO}_2^+ + \text{H}_3\text{O}^+ + 2\text{HSO}_4^-$ for sulfuric acid and $\text{HNO}_3 + 2\text{HClO}_4 \rightarrow \text{NO}_2^+ + \text{H}_3\text{O}^+ + 2\text{ClO}_4^-$ for perchloric acid.^[49] Importantly, the experiment by Gerber et al.^[46] revealed that more HNO_3 is dissociated to form more NO_2^+ ions if a greater quantity of its complementary acid is added. This may explain the increased consumption of CNTs as the fraction of HClO_4 was increased during reflux with the $\text{HClO}_4/\text{HNO}_3$ mixture. Furthermore, involvement of water in the reaction suppresses NO_2^+ formation: greater than 50 mol% water causes zero dissociation in HNO_3 .^[47] Thus, the $\text{HClO}_4/\text{f-HNO}_3$ (3:1) mixture consumes CNTs completely by formation of a greater quantity of nitronium ions.

For all 11 reflux solutions listed in Figure 3b, the Fe concentrations measured by UV/Vis spectroscopy were in good agreement with those measured using ICP-OES within an average difference of 6.0%. Therefore, the colorimetric method developed in this study using UV/Vis spectroscopy appears to be a reliable tool for accurate measurement of Fe concentrations in acid refluxed solutions of CNTs.

In an attempt to demonstrate its reliability, this method was applied to other CNT samples, namely CNT-B and CNT-C. Both CNTs were synthesized using Fe and Co catalysts on alumina supports by catalytic chemical vapor deposition (CCVD). In Fig-

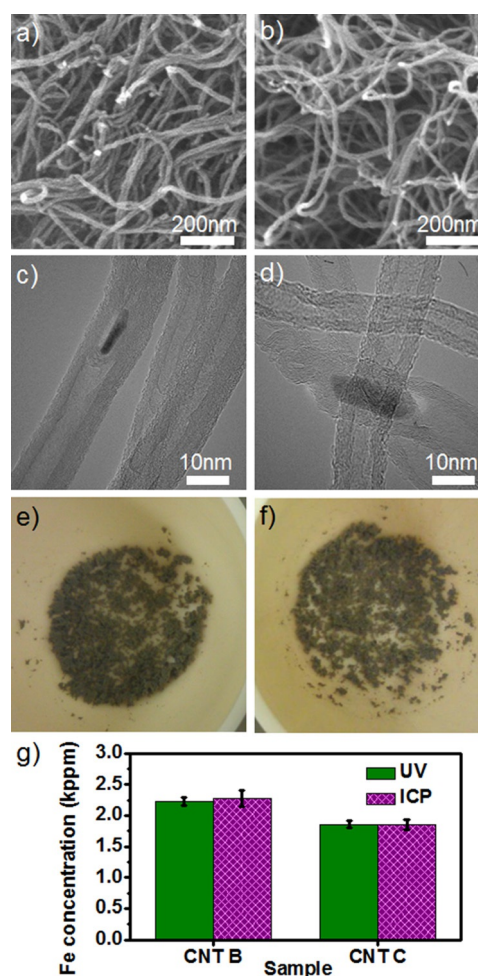


Figure 4. SEM images of a) CNT-B and b) CNT-C. TEM images of c) CNT-B and d) CNT-C show that multiple graphitic layers encase catalyst particles. The ashes, produced by oxidizing CNTs at 900°C , have a grey color for both e) CNT-B and f) CNT-C. g) Fe concentrations measured by UV/Vis spectroscopy and ICP-OES for CNT-B and CNT-C. Data are the average \pm SD of three independent measurements.

ure 4a–d, CNTs occurred entangled, and metal catalysts were enclosed by CNTs for both CNT-B and -C. The ashes, obtained by burning at 900°C in air, appeared grey because Fe and Co were used as catalysts (Figure 4e,f). Fe measurements were made three times for each CNT sample using UV/Vis spectroscopy and ICP-OES (Figure 4g). Fe concentrations measured by both methods closely match each other within the average differences of 1.66 and 0.38% for CNT-B and -C, respectively, supporting that the UV/Vis spectroscopic method is comparable to the widely used ICP-OES technique in assessing the Fe content of CNTs. Measurement precision, as indicated by the small error bars, illustrates the reliability of this method.

Conclusions

Easy-to-use and widely available UV/Vis spectroscopy was used to determine the concentration of Fe catalysts in CNTs by formation of colored complexes with the 1,10-phenanthroline (phen) ligand. This colorimetric method revealed a linear rela-

tionship between Fe concentration and optical absorbance of the CNT refluxed solution. An unknown concentration of Fe was calculated by fitting its corresponding absorbance to the linear equation. CNTs were held at reflux in a variety of single and mixed acids to compare their capacity to extract Fe from CNTs, so that Fe catalysts encapsulated by CNTs or graphitic layers could be fully dissolved. Among the single or mixed acids considered, mixtures of H₂SO₄/HNO₃ (3:1), HClO₄/HNO₃ (1:1), HClO₄/HNO₃ (3:1), and HClO₄/f-HNO₃ (3:1) exhibited the strongest dissolution capacity for Fe. With regard to the refluxed solutions, Fe concentrations measured by UV/Vis spectroscopy and ICP-OES were in good agreement with each other, indicating that our colorimetric method using UV/Vis spectroscopy is reliable and applicable to the assessment of Fe content in CNTs.

Experimental Section

Materials: CNTs provided by JEIO Company (Korea) were multi-walled synthesized by CCVD. The specifications of these CNTs are listed in Table 1. Reagents used for Fe determination were purchased from Sigma–Aldrich: hydroxylamine hydrochloride (NH₂OH·HCl, 99%), 1,10-phenanthroline (C₁₂H₈N₂, ≥99%), ammoni-

Table 1. Specification of CNTs used for Fe content measurements.

CNT	Catalyst	Ash content [%]	∅ [nm]	<i>I_d/I_g</i>
CNT-A	Fe on Al	3.51 ± 0.03	15.5 ± 4.8	0.757 ± 0.04
CNT-B	Fe and Co on Al	1.27 ± 0.05	17.3 ± 6.8	0.634 ± 0.02
CNT-C	Fe and Co on Al	1.12 ± 0.03	11.6 ± 3.0	0.0683 ± 0.03

um iron(II) sulfate hexahydrate ([Fe(NH₄)₂(SO₄)₂·6H₂O]), 99.997%), acetic acid (CH₃COOH, ≥99.9%), and sodium hydroxide (NaOH, ≥97%). Fe flakes (99.99%) and aluminum (Al) pellets (99.999%) purchased from LTS Chemicals (Chestnut Ridge, NY, USA) were used for validation. The concentrated acids used to extract Fe components from CNTs and ashes were hydrochloric acid (HCl, ~35%, Daejung), nitric acid (HNO₃, ~70%, Daejung), fumed nitric acid (f-HNO₃, ~93%, Matsunoen), sulfuric acid (H₂SO₄, 95–98%, Sigma–Aldrich), and perchloric acid (HClO₄, ~70%, Sigma–Aldrich). All chemicals were used as received. Ash was prepared by completely burning CNTs in air at 900 °C.

An Fe standard solution with an Fe concentration of 500 ppm was made by dissolving [Fe(NH₄)₂(SO₄)₂·6H₂O] (0.3509 g) in H₂SO₄ (0.25 mL) in a 100 mL volumetric flask and then diluting with distilled water. A sodium acetate (CH₃COONa) buffer solution was prepared by mixing 6 M CH₃COOH (100 mL) with 5 M NaOH (100 mL). Aqueous solutions of hydroxylamine (10 wt%) and o-phen (0.1 wt%) were prepared at room temperature and 60 °C, respectively.

A classical colorimetric method for Fe determination has been described elsewhere,^[34,35] and the procedure was modified here for sample preparation. A series of Fe solutions was obtained by diluting the 500 ppm Fe standard solution: 0, 0.2, 0.6, 1, 1.4, and 1.8 mL standard solutions of 500 ppm were added to 100 mL volumetric flasks to produce calibration solutions with Fe concentrations of 0,

1, 3, 5, 7, and 9 ppm, respectively. Subsequently, sodium acetate buffer (8 mL), hydroxylamine solution (1 mL), and o-phen solution (10 mL) in turn were added at intervals of 10 min between each solution. Distilled water was added to make up 100 mL calibration solutions.

To determine whether the presence of Al in solution influenced the accuracy of Fe determination, a validation process was carried out. We prepared five solutions at various Fe and Al ratios while maintaining the total concentration of these ions at 10 ppm, as described below. Individual stock solutions for Fe and Al were separately produced by dissolving Fe flakes (0.0525 g) and Al pellets (0.0560 g) in concentrated HCl, respectively. Mixtures with different ratios of Fe and Al stock solutions were prepared, and buffer solution, hydroxylamine solution, and o-phen solution were subsequently added.

To prepare solution samples for Fe determination, the CNTs (60 mg) or ashes (15 mg) were held at reflux with acid (10 mL) in an oil bath maintained at 130 °C. Next, the acid mixture was filtered, and the filtrate was collected in a 100 mL volumetric flask. The filtrates, with volumes of 5 and 1 mL for CNTs and ashes, respectively, were transferred to a 50 mL volumetric flask. Buffer solution, hydroxylamine solution, and o-phen solution were added, and distilled water was finally added to bring the volume to 50 mL, developing red–orange colored solutions for spectroscopic measurement of Fe content. The optical absorbance used to determine Fe content was assessed not only based on the red–orange colored Fe–phen complexes, but also by the reagents contained in the solution, such as CNTs. Blank solutions for correction of spectroscopic measurements were prepared by following the same procedure as that followed for calibration samples, mixing the same amounts of all reagents including the CNTs, but omitting phen to prohibit the formation of red–orange colored Fe–phen complexes.

Characterization: CNTs were characterized using field emission scanning electron microscopy (FE-SEM, Hitachi S-4700) and high-resolution transmission electron microscopy (HRTEM, Tecnai G2 F20) to observe their morphologies and structures. Raman spectroscopy (Renishaw System 3000, laser λ = 633 nm) was used to characterize the crystalline nature and structural defects in CNTs. The oxidation temperature of CNTs was measured by thermogravimetric analysis (STA S-1500). Inductively coupled plasma optical emission spectrometry (ICP-OES, PerkinElmer OPTIMA 4300 DV) was used to measure metal impurity content in the CNT or ash samples by examining the specific wavelengths of λ = 238.204 and 396.153 nm, corresponding to Fe and Al, respectively. The solution for ICP-OES analysis was typically prepared by boiling the sample in a closed Teflon vessel with aqua regia (HCl/HNO₃ = 3:1) at 200 °C for 1 day and then cooling to room temperature. After the solvent was evaporated, the residue was diluted with 2% nitric acid solution before measurement.

The absorbance values of the solutions prepared for Fe determination were measured by UV/Vis–near infrared spectroscopy (UV/Vis–NIR spectrophotometer, Agilent, Cary 5000) in the spectral range of λ = 400–600 nm. The peak absorbance value was recorded at λ = 510 nm for the Fe–phen complexes. A fitting equation was obtained by plotting the peak absorbance values versus Fe concentrations, and was used to determine the Fe concentration for an unknown sample.

Acknowledgements

This work was supported by the Industrial Strategic Technology Development Program (No. 10041851) funded by the Ministry of Trade, Industry & Energy (MOTIE), Korea and supported by the Individual Basic Science & Engineering Research Program (NRF-2013R1A1A2010551) funded by the National Research Foundation of Korea.

Keywords: acid treatment • iron catalysts • nanotubes • phenanthroline • UV/Vis spectroscopy

- [1] P. Kim, L. Shi, A. Majumdar, P. L. McEuen, *Phys. Rev. Lett.* **2001**, *87*, 215502.
- [2] R. H. Baughman, A. A. Zakhidov, W. A. de Heer, *Science* **2002**, *297*, 787–792.
- [3] B. Q. Wei, R. Vajtai, P. M. Ajayan, *Appl. Phys. Lett.* **2001**, *79*, 1172–1174.
- [4] T.-W. Chou, L. Gao, E. T. Thostenson, Z. Zhang, J.-H. Byun, *Compos. Sci. Technol.* **2010**, *70*, 1–19.
- [5] A. Izadi-Najafabadi, T. Yamada, D. N. Futaba, M. Yudasaka, H. Takagi, H. Hatori, S. Iijima, K. Hata, *ACS Nano* **2011**, *5*, 811–819.
- [6] M. F. L. De Volder, S. H. Tawfick, R. H. Baughman, A. J. Hart, *Science* **2013**, *339*, 535–539.
- [7] M. Kumar, Y. Ando, *J. Nanosci. Nanotechnol.* **2010**, *10*, 3739–3758.
- [8] A. M. Cassell, J. A. Raymakers, J. Kong, H. Dai, *J. Phys. Chem. B* **1999**, *103*, 6484–6492.
- [9] Y. Ando, X. Zhao, T. Sugai, M. Kumar, *Mater. Today* **2004**, *7*, 22–29.
- [10] C. L. Pint, S. T. Pheasant, M. Pasquali, K. E. Coulter, H. K. Schmidt, R. H. Hauge, *Nano Lett.* **2008**, *8*, 1879–1883.
- [11] B. Šljukić, C. E. Banks, R. G. Compton, *Nano Lett.* **2006**, *6*, 1556–1558.
- [12] K.-U. Jeong, J. Y. Lim, J.-Y. Lee, S. L. Kang, C. Nah, *Polym. Int.* **2010**, *59*, 100–106.
- [13] M. Pumera, Y. Miyahara, *Nanoscale* **2009**, *1*, 260–265.
- [14] P. Gayathri, A. S. Kumar, *Chem. Eur. J.* **2013**, *19*, 17103–17112.
- [15] F. Wei, Q. Zhang, W.-Z. Qian, H. Yu, Y. Wang, G.-H. Luo, G.-H. Xu, D.-Z. Wang, *Powder Technol.* **2008**, *183*, 10–20.
- [16] W. Huang, Y. Wang, G. Luo, F. Wei, *Carbon* **2003**, *41*, 2585–2590.
- [17] T.-J. Park, S. Banerjee, T. Hemraj-Benny, S. S. Wong, *J. Mater. Chem.* **2006**, *16*, 141–154.
- [18] E. F. Antunes, V. G. de Resende, U. A. Mengui, J. B. M. Cunha, E. J. Corat, M. Massi, *Appl. Surf. Sci.* **2011**, *257*, 8038–8043.
- [19] A. Senthil Kumar, P. Gayathri, P. Barathi, R. Vijayaraghavan, *J. Phys. Chem. C* **2012**, *116*, 23692–23703.
- [20] L. P. Biró, N. Q. Khanh, Z. Vértesy, Z. E. Horváth, Z. Osváth, A. Koós, J. Gyulai, A. Kocsonya, Z. Kónya, X. B. Zhang, G. Van Tendeloo, A. Fonseca, J. B. Nagy, *Mater. Sci. Eng. C* **2002**, *19*, 9–13.
- [21] C. Ge, F. Lao, W. Li, Y. Li, C. Chen, Y. Qiu, X. Mao, B. Li, Z. Chai, Y. Zhao, *Anal. Chem.* **2008**, *80*, 9426–9434.
- [22] T. Braun, H. Rausch, L. P. Biró, Z. Konya, I. Kiricsi, *J. Radioanal. Nucl. Chem.* **2004**, *262*, 31–34.
- [23] K. X. Yang, M. E. Kitto, J. P. Orsini, K. Swami, S. E. Beach, *J. Anal. At. Spectrom.* **2010**, *25*, 1290–1297.
- [24] D. Harvey, *Modern Analytical Chemistry*, McGraw-Hill, New York, NY, **1999**, pp. 380–409.
- [25] H. Pyenson, P. H. Tracy, *J. Dairy Sci.* **1945**, *28*, 401–412.
- [26] M. S. Karacan, N. Aslantaş, *J. Hazard. Mater.* **2008**, *155*, 551–557.
- [27] D. Y. Yegorov, A. V. Kozlov, O. A. Azizova, Y. A. Vladimirov, *Free Radical Biol. Med.* **1993**, *15*, 565–574.
- [28] A. Apilux, W. Dungchai, W. Siangproh, N. Praphairaksit, C. S. Henry, O. Chailapakul, *Anal. Chem.* **2010**, *82*, 1727–1732.
- [29] C. Nan, L. Ni, L. Yang, W. Shuangfei, *World Automation Congress (WAC) 2012*, **2012**, 1–3.
- [30] L. Goldstein, Z.-P. Teng, E. Zeserson, M. Patel, R. F. Regan, *J. Neurosci. Res.* **2003**, *73*, 113–121.
- [31] P. Gayathri, A. Senthil Kumar, *Langmuir* **2014**, *30*, 10513–10521.
- [32] H. Irving, D. H. Mellor, *J. Chem. Soc.* **1962**, 5237–5245.
- [33] T. S. Lee, I. M. Kolthoff, D. L. Leussing, *J. Am. Chem. Soc.* **1948**, *70*, 2348–2352.
- [34] H. Tamura, K. Goto, T. Yotsuyanagi, M. Nagayama, *Talanta* **1974**, *21*, 314–318.
- [35] L. G. Saywell, B. B. Cunningham, *Ind. Eng. Chem. Anal. Ed.* **1937**, *9*, 67–69.
- [36] T. Asami, K. Kumada, *Soil Sci. Plant Nutr.* **1960**, *5*, 179–183.
- [37] G. G. Rao, G. Somidevamma, *Fresenius Z. Anal. Chem.* **1959**, *165*, 432–436.
- [38] H. Fadrus, J. Maly, *Analyst* **1975**, *100*, 549–554.
- [39] W. B. Fortune, M. G. Mellon, *Ind. Eng. Chem. Anal. Ed.* **1938**, *10*, 60–64.
- [40] A. E. Harvey, J. A. Smart, E. S. Amis, *Anal. Chem.* **1955**, *27*, 26–29.
- [41] K. L. Strong, D. P. Anderson, K. Lafdi, J. N. Kuhn, *Carbon* **2003**, *41*, 1477–1488.
- [42] W. A. Tilden, *J. Chem. Soc.* **1874**, *27*, 630–636.
- [43] ISO 17025, Switzerland, **2005**, 10–23.
- [44] Y.-R. Shin, I.-Y. Jeon, J.-B. Baek, *Carbon* **2012**, *50*, 1465–1476.
- [45] A. Pistone, A. Ferlazzo, M. Lanza, C. Milone, D. Iannazzo, A. Piperno, E. Piperopoulos, S. Galvagno, *J. Nanosci. Nanotechnol.* **2012**, *12*, 5054–5060.
- [46] I. Gerber, M. Oubenali, R. Bacsá, J. Durand, A. Gonçalves, M. F. R. Pereira, F. Jolibois, L. Perrin, R. Poteau, P. Serp, *Chem. Eur. J.* **2011**, *17*, 11467–11477.
- [47] H. G. M. Edwards, V. Fawcett, *J. Mol. Struct.* **1994**, *326*, 131–143.
- [48] E. S. Halberstadt, E. D. Hughes, C. K. Ingold, *Nature* **1946**, *158*, 514.
- [49] C. K. Ingold, D. J. Millen, H. G. Poole, *J. Chem. Soc.* **1950**, 2576–2589.

Received: April 14, 2015

Published online on June 29, 2015